Optical properties of shallow tropical cumuli derived from ARM ground-based remote sensing

S. A. McFarlane[1] and W. W. Grabowski[2]

Received 13 November 2006; revised 8 January 2007; accepted 6 February 2007; published 28 March 2007.

[1] This paper presents results from ground-based remote sensing of optical properties of shallow convective clouds over the Nauru ARM site using the technique developed by McFarlane et al. (2002). Herein, the results of a pilot study are presented with analysis of about six months of cloud data. The effective radius r_e shows large spatial variability, with the frequency of occurrence relatively narrow near the cloud base, and gradually widening aloft. Available column data for LWC and r_e allow derivation of the pdf of the optical thickness τ. The pdf shows that clouds with τ in the range 5 to 10 are most frequent, but there is a long tail with clouds up to τ = 100. These results are discussed in the context of traditional observations of cloud microstructure using an instrumented aircraft. **Citation:** McFarlane, S. A., and W. W. Grabowski (2007), Optical properties of shallow tropical cumuli derived from ARM ground-based remote sensing, *Geophys. Res. Lett.*, *34*, L06808, doi:10.1029/2006GL028767.

1. Introduction

[2] The local liquid water content (LWC) and the shape of the cloud droplet spectrum (the latter represented by the effective radius r_e, the ratio between the third and the second moment of the droplet spectrum) [*Stephens*, 1978] determine local optical properties of ice-free clouds, such as subtropical stratocumulus and trade-wind cumulus. The optical thickness, the single-scattering albedo, and the asymmetry factor can all be parameterized as a function of the cloud depth, LWC and r_e [e.g., *Stephens*, 1978; *Slingo and Schrecker*, 1982; *Hu and Stamnes*, 1993]. Spatial distribution of these properties controls the area-averaged albedo of a cloud field. Stratocumulus and cumulus clouds are significantly diluted by entrainment of dry environmental air [e.g., *Stommel*, 1947; *Warner*, 1955; *Blyth*, 1993; *Chosson et al.*, 2007], which has significant impact on cloud optical properties. For LWC, its dilution is determined by the conservation of the total water and the moist static energy. Predicting changes of the cloud droplet spectrum, on the other hand, requires additional constraints. This is because conservation of water and energy does not allow distinguishing between situations where cloud water after homogenization is distributed over either the same number of smaller droplets (i.e., the homogeneous mixing scenario) or a smaller number of droplets all with the initial size (i.e., the extremely inhomogeneous mixing scenario [*Baker et al.*, 1980]; see discussion by *Andrejczuk et al.* [2006] and *Burnet and Brenguier* [2007]). This is an important issue because the assumptions about the impact of entrainment and mixing on cloud droplet spectra have been shown to significantly affect mean radiative properties of a field of stratocumulus and cumulus clouds [*Chosson et al.*, 2004, 2007; *Grabowski*, 2006].

[3] Microphysical properties of various clouds and cloud systems are typically investigated using aircraft instrumented with optical probes capable of providing spectra of cloud droplets and rain/drizzle drops averaged over a distance of tens of meters or shorter along the flight track [see *Burnet and Brenguier*, 2007, and references therein]. Using this information, LWC and r_e can be derived from the observed spectra [e.g., *Stephens and Platt*, 1987; *Martin et al.*, 1994; *Pawlowska and Brenguier*, 2000]. *Blyth and Latham* [1991] showed that in Montana cumuli observed during the 1981 CCOPE (Cooperative Convective Precipitation Experiment) r_e only weakly depended on the adiabatic fraction (AF), the ratio between the LWC and its adiabatic value. This seems consistent with the extremely inhomogeneous mixing scenario. Such a scenario is also consistent with droplet spectral changes observed in many traverses across small continental cumuli during the SCMS (Small Cumulus Microphysics) experiment [*Gerber*, 2000] and in traverses in actively growing trade-wind cumulus turrets during RICO (Rain in Cumulus over the Ocean) [*Gerber*, 2006]. In some RICO cases, however, spectral changes were argued to result from the nucleation of fresh cloud droplets due to entrainment. Similar results were reported earlier by *Pontikis and Hicks* [1993]. *Heymsfield and McFarquhar* [2001, Figure 6] reported wide frequency distributions of the effective radius from cloud penetrations during long-distance cross-equatorial flights in INDOEX (Indian Ocean Experiment).

[4] This paper reports results from ground-based observations over the ARM (Atmospheric Radiation Measurement, see www.arm.gov) Tropical Western Pacific Nauru site (0.5S, 166.9E) using the technique developed by *McFarlane et al.* [2002]. The island of Nauru is located in the equatorial central Pacific and typical low-level cloudiness consists of fields of shallow trade-wind cumuli. Although one can argue that ground-based remote sensing of cloud optical properties has significant uncertainties (see a brief discussion below), its main advantage is an unprecedented length of the record (i.e., sampling of many clouds that pass overhead). Moreover, ground-based remote sensing provides instantaneous vertical profiles of cloud optical properties, which, unlike aircraft observations, can be directly applied as input to two-stream independent-column-approximation radiative transfer models, typically used in the clouds-in-climate problem [e.g., *Grabowski*, 2006, and references therein]. However, the low spatial resolution of ground-based remote sensing compared to

[1]Pacific Northwest National Laboratory, Richland, Washington, USA.
[2]National Center for Atmospheric Research, Boulder, Colorado, USA.

0094-8276/07/2006GL028767

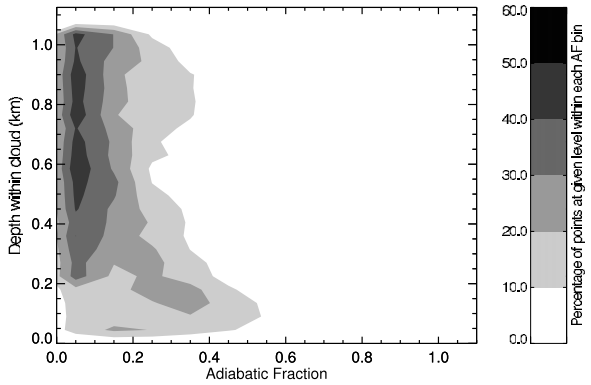

Figure 1. CFAD of the adiabatic fraction (AF) for the entire data set analyzed in this study. CFAD is calculated using 0.1 as AF bin width.

aircraft observations has to be kept in mind. The next section briefly discusses the technique used in this study. Results are presented in section 3 and their brief discussion in section 4 concludes the paper.

2. Measurements, Data Set, and Numerical Procedures

[5] Vertical profiles of r_e and LWC for boundary layer clouds at Nauru are retrieved from microwave radiometer (MWR) brightness temperatures and millimeter cloud radar (MMCR) reflectivity using the Bayesian retrieval algorithm developed by *McFarlane et al.* [2002], which combines prior information on cloud microphysics with remote sensing observations. Prior probability density functions for liquid water clouds were derived from the second, third, and sixth moments of the droplet size distributions measured by in situ aircraft probes in shallow cumuli during the JHWRP (Joint Hawaiian Warm Rain Project) and SCMS field experiments (see *McFarlane et al.* [2002] for further discussion). These were combined with forward models for radar reflectivity and microwave brightness temperatures to retrieve the posterior pdf within the Bayesian framework. We integrate over the posterior pdf to calculate the mean vertical profile and the variance around the mean, which is an estimate of the uncertainty in the retrieval. Unlike other radar-radiometer retrievals [e.g., *Frisch et al.*, 1995], no assumptions about the form of the droplet size distribution are made, uncertainties on the input measurements are included, and uncertainty estimates on the retrieved properties are returned. Analysis of the retrieval using large eddy simulations of maritime trade cumulus cloud fields found root-mean-square (RMS) errors of 2.0–3.3 μm in r_e and 0.14–0.19 gm^{-3} in LWC [*McFarlane et al.*, 2002]. The RMS errors in r_e were significantly smaller than those retrieved from the *Frisch et al.* [1995] algorithm, while the LWC errors were comparable. It needs to be emphasized, however, that no aircraft observations are available to validate the retrievals presented in this paper.

[6] The MMCR is a vertically pointing Doppler radar operating at 34.86 GHz [*Clothiaux et al.*, 1999]. In this analysis, we use data only from the boundary layer mode, which has a minimum signal of −60 dBZ at 1 km and 45 m vertical resolution. In the current configuration, sampling occurs approximately every 40 seconds, over a 9 second interval. Given typical wind speeds of 8.4 m/s at Nauru [*McFarlane and Evans*, 2004], the horizontal resolution of each radar measurement due to the sampling time is about 77 m. *Kollias et al.* [2005] compared the MMCR Doppler moment estimates for Florida cumulus to those from a radar with 2-s sampling and determined that the Doppler moments from the two radars were highly correlated, except in cases of high turbulence. The MWR is a dual-channel radiometer operating at wavelengths of 23.8 GHz and 31.4 GHz. Brightness temperatures are reported at 20 s resolution and are interpolated to match the radar times. In summary, the retrievals provide information on spatial variability of LWC and r_e on scales ∼100 m, which is relatively low when compared to modern aircraft observations [cf. *Gerber*, 2000, 2006; *Burnet and Brenguier*, 2007], but similar to the photon mean free path inside a cloud.

[7] We perform retrievals on approximately 6 months of data (16 June 1999 – 19 December 1999) at Nauru. Over 34,000 profiles occurring within 3 hours of a radiosonde launch were found to contain clouds with radar cloud base (lowest radar range gate with reflectivity greater than −60 dBZ) less than 2000 m. To reduce cloud edge effects, we restrict the analysis to profiles with at least 5 consecutive range gates (i.e., 225 m thick) having reflectivity greater than −60 dBZ. To reduce the potential for sampling clouds containing precipitation or drizzle, we require the maximum radar reflectivity in the cloud to be less than −10 dBZ, and the radar cloud base to be within 100 m of cloud base determined from a laser ceilometer at the site. Approximately 30% of the radar profiles containing cloud were removed due to the cloud thickness limitation and about 60% of the profiles were removed due to potential drizzle contamination. Overall, the above restrictions resulted in retrievals of r_e and LWC profiles only for clouds with depths between approximately 200 m and 1 km.

[8] Local values of the adiabatic fraction AF are estimated using the retrieved LWC and profiles of the adiabatic LWC, the latter estimated from the analysis of the adiabatic parcel raising from the observed cloud base. Parcel analysis assumes that cloud base represents raising boundary layer air that is exactly at water saturation and that cloud-base temperature can be approximated by the environmental temperature at this level from the nearest in-time air sounding.

3. Results

[9] Figure 1 presents the contoured frequency by altitude diagram (CFAD) of the adiabatic fraction AF in all clouds for the period selected. When observed with an instrument capable of only resolving spatial scales of ∼100 m, small Cu above the Nauru site appear strongly diluted, with AF reaching only about half near the cloud base and decreasing to about 0.1 near the typical maximum cloud depth of 1 km. (See *Gerber* [2000, Figure 2], who illustrates the impact of the spatial resolution of cloud measurements on the estimate of cloud dilution.) When the entire data set is divided into subsets of clouds with different cloud top heights (not shown), it is apparent that deeper clouds have higher cloud-base AF and that AF rapidly decreases with height

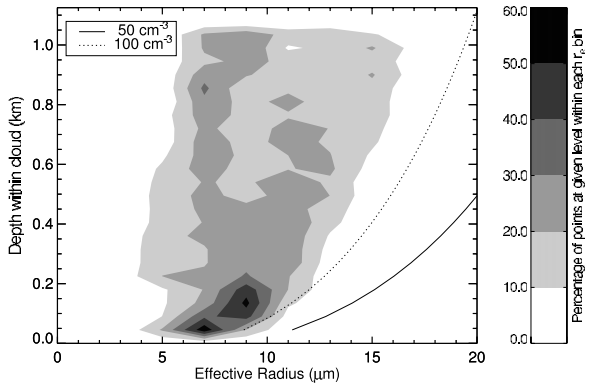

Figure 2. CFAD of the effective radius using 2 μm wide bins for the same clouds as in Figure 1. Effective radius for adiabatic clouds with droplet concentrations of 50 and 100 cm^{-3} are shown by solid and dashed lines, respectively.

in all subsets, from the highest value near the cloud base to values around 0.1 near the cloud top. In general, the rapid decrease of AF with height is reminiscent of the profiles obtained from similar-spatial-resolution aircraft observations of shallow convective clouds reported in *Warner* [1955].

[10] Figure 2 shows the CFAD of r_e. For reference, adiabatic r_e corresponding to droplet concentrations of 50 and 100 cm^{-3} are also shown, assuming that r_e and the mean volume radius r_v are related as $r_v^3 = kr_e^3$, where $k \approx 0.80$ for maritime conditions (*Martin et al.*, 1994). Such a range of droplet concentrations can be thought of as typical for the pristine marine environment of the equatorial central Pacific (e.g., see concentrations observed in trade wind cumuli off Australia reported by *Stephens and Platt* [1987]). The effective radius sharply increases in the first couple hundred meters above the cloud base, reflecting rapid growth of cloud droplets nucleated at the base by diffusion of water vapor. After a few hundred meters, however, the CFAD shows a transition into a wide bimodal shape, arguably reflecting a wide range of mixing scenarios and possibly fresh nucleation of cloud droplets due to entrainment of environmental dry air into a cloud. The peak at large values, reaching about 15 μm near the cloud top, represents droplets with radii several microns smaller than the adiabatic values. Since the air near the cloud top is on average strongly diluted (see Figure 1), this peak represents droplet spectral transformations which resemble intermediate mixing (i.e., between homogeneous and extremely inhomogeneous, with reduction of both the droplet radius and droplet concentration). The peak at small sizes, on the other hand, corresponds to droplet sizes not much different than those observed near the cloud base. Arguably, some of these droplets come from fresh nucleation above the cloud base. There are many cases where r_e falls between the two peaks.

[11] Figure 3 shows examples of the relationship between r_e and AF for clouds with two different ranges of liquid water paths (LWPs; 10–50 and 100–500 g m^{-2}, i.e., with different cloud top heights) at two different heights above the cloud base, corresponding roughly to one-third and two-thirds of their typical depths. As in Figure 2, r_e corresponding to the LWC for a given adiabatic fraction and assuming droplet concentrations of 50 and 100 cm^{-3} are also shown. The ranges of r_e in various panels roughly agree with the ranges shown in Figure 2 (e.g., from 5 to 10 μm at 100 m above the cloud base; 5 to 15 μm at 600 m). At very low AF, r_e follows the droplet size for the concentration of about 50 cm^{-3}. Data points with AFs larger than 0.4 are present only at lower levels for both types of clouds (left panels in Figure 3). These diagrams do not seem to show the tendency of r_e to be independent of AF as observed by *Blyth and Latham* [1991] and *Gerber* [2000].

[12] Finally, Figure 4 shows the pdf of the optical thickness calculated from profiles of the LWC and r_e assuming no absorption of solar radiation for all cloud profiles included in the present study. The optical thickness of each column is calculated as $\tau = \frac{3}{2}\frac{1}{\rho_w}\int_0^H \frac{\mathrm{LWC}}{r_e}dz$, where ρ_w is the water density [cf. *Stephens*, 1978; *Grabowski*, 2006]. The plot shows that the optical thickness between 5 and 10 is the most frequent which attests to the highly diluted nature of shallow clouds above the Nauru site. A long tail up to $\tau = 100$ is also apparent.

4. Discussion and Conclusions

[13] Optical properties of shallow warm clouds, such as stratocumulus and shallow cumulus, play an important role in the Earth's radiative balance. Such clouds are more

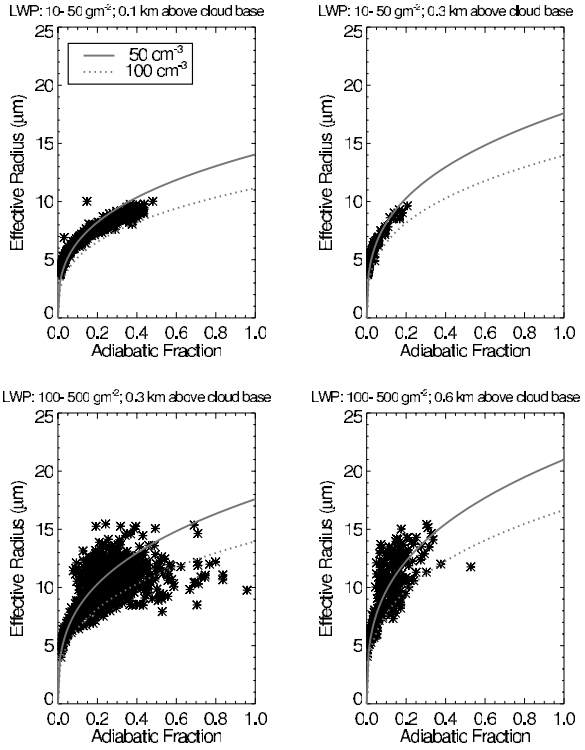

Figure 3. Effective radius versus AF for (top) shallow clouds (LWP between 10 and 50 g m^{-2}) and (bottom) deeper clouds (LWP between 100 and 500 g m^{-2}). Data for (top left) 0.1 km, (top right and bottom left) 0.3 km, and (bottom right) 0.6 km above the cloud base. Effective radius for LWC corresponding to a given AF and for droplet concentration of 50 and 100 cm^{-3} are shown by solid and dashed lines, respectively.

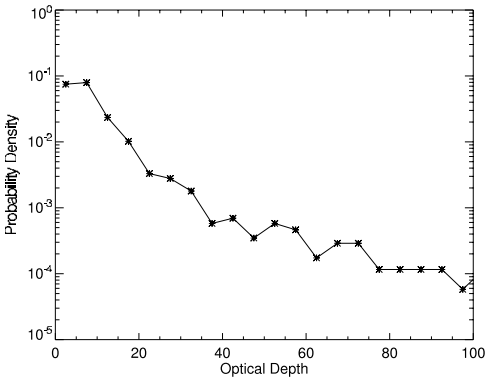

Figure 4. Pdf of the cloud optical thickness for all clouds included in this study.

important than deep clouds because the reflection of solar radiation by shallow clouds far outweighs their effect on the thermal radiation. The LWC and r_e are the key parameters for representing the optical properties of these clouds. Because these clouds are significantly diluted by entrainment, understanding the microphysical transformations resulting from cloud dilution is the key issue [*Chosson et al.*, 2004, 2007; *Grabowski*, 2006]. The data shown in this paper provide insights into bulk optical properties of these clouds, thus complementing aircraft observations that have been used previously to investigate the impact of entrainment and mixing on the cloud droplet spectra (see discussion by *Burnet and Brenguier* [2007, and references therein]). Remote sensing of shallow clouds over the Nauru site provides an unprecedented volume of data, only a small fraction of which was analyzed in this study.

[14] Some of the results presented here merely confirm well-known facts. For instance, the fact that shallow Cu are significantly diluted is well known since the pioneering aircraft observations by *Stommel* [1947] and *Warner* [1955], and it has been confirmed in many subsequent observational studies, especially when only low-spatial-resolution observations are available [cf. *Gerber*, 2000, Figure 2]. The shape of the CFAD of r_e presented in Figure 2 also seems consistent with previous theoretical and observational studies [e.g., *Warner*, 1969; *Paluch and Knight*, 1984; *Pontikis and Hicks*, 1993; *Brenguier and Grabowski*, 1993; *Su et al.*, 1998; *Heymsfield and McFarquhar*, 2001]. The results support the view that shallow cumuli are very inhomogeneous as far as their microphysical properties are concerned. CFADs of r_e are wide, with the width increasing with height, and show peaks at limits corresponding to the size significantly smaller than the adiabatic value and the size corresponding to droplets after recent nucleation. Such wide distributions, combined with the distributions of LWC, lead to a wide pdf of the observed optical thickness τ (Figure 4), with maximum frequency for τ in the 5 to 10 range and a long tail extending beyond $\tau = 100$. Whether the latter is true for various environmental conditions remains to be seen. Although the conditions over the Nauru site are quite steady during this study period, there exist periods with significantly different conditions, e.g., due to differences between El-Niño and La-Niña years. Analysis of the data from these different periods and/or from other ARM sites might turn out to be very useful in the development of robust parameterizations of optical properties of shallow ice-free clouds. Observations reported here should also be used in validating large-eddy simulation models, which are typically used in studies concerning these shallow clouds. We hope to present results of such investigations in the future.

[15] **Acknowledgments.** This work was supported by the Office of Biological and Environmental Research of the U.S. Department of Energy under contract DE-AC06-76RL01830 as part of the Atmospheric Radiation Measurement Program (McFarlane) and by NOAA grant NA05OAR4310107 (Grabowski).

References

Andrejczuk, M., W. W. Grabowski, S. P. Malinowski, and P. K. Smolarkiewicz (2006), Numerical simulation of cloud-clear air interfacial mixing: Effects on cloud microphysics, *J. Atmos. Sci.*, *63*, 3204–3225.

Baker, M. B., R. G. Corbin, and J. Latham (1980), The influence of entrainment on the evolution of cloud droplet spectra: I. A model of inhomogeneous mixing, *Q. J. R. Meteorol. Soc.*, *106*, 581–598.

Blyth, A. M. (1993), Entrainment in cumulus clouds, *J. Appl. Meteorol.*, *32*, 626–640.

Blyth, A. M., and J. Latham (1991), A climatological parameterization for cumulus clouds, *J. Atmos. Sci.*, *21*, 2367–2371.

Brenguier, J.-L., and W. W. Grabowski (1993), Cumulus entrainment and cloud droplet spectra: A numerical model within a two-dimensional dynamical framework, *J. Atmos. Sci.*, *50*, 120–136.

Burnet, F., and J. L. Brenguier (2007), Observational study of the entrainment-mixing process in warm convective clouds, *J. Atmos. Sci*, in press.

Chosson, F., J.-L. Brenguier, and M. Schröder (2004), Radiative impact of mixing processes in boundary layer clouds, paper presented at International Conference on Clouds and Precipitation, Int. Comm. on Clouds and Precip., Bologna, Italy.

Chosson, F., J.-L. Brenguier, and L. Schüller (2007), Entrainment-mixing and radiative transfer simulation in boundary-layer clouds, *J. Atmos. Sci.*, in press.

Clothiaux, E. E., K. P. Moran, B. E. Martner, T. P. Ackerman, G. G. Mace, T. Uttal, J. H. Mather, K. B. Widener, M. A. Miller, and D. J. Rodriguez (1999), The Atmospheric Radiatiom Measurement Program cloud radars: Operational modes, *J. Atmos. Oceanic Technol.*, *16*, 819–827.

Frisch, A. S., C. W. Fariall, and J. B. Snider (1995), Measurements of stratus cloud and drizzle parameters in ASTEX with a Ka-band Doppler radar and a microwave radiometer, *J. Atmos. Sci.*, *52*, 2788–2799.

Gerber, H. (2000), Structure of small cumulus clouds, paper presented at 13th International Conference on Clouds and Precipitation, Int. Comm. on Clouds and Precip., Reno, Nev.

Gerber, H. (2006), Entrainment, mixing, and microphysics in RICO cumulus, paper presented at 12th AMS Conference on Cloud Physics, Am. Meteorol. Soc., Madison, Wis. (Available at http://ams.confex.com/ams/htsearch.cgi.)

Grabowski, W. W. (2006), Indirect impact of atmospheric aerosols in idealized simulations of convective-radiative quasi-equilibrium, *J. Clim.*, *19*, 4664–4682.

Heymsfield, A. J., and G. M. McFarquhar (2001), Microphysics of INDOEX clean and polluted trade cumulus clouds, *J. Geophys. Res.*, *106*(D22), 28,653–28,674.

Hu, Y. X., and K. Stamnes (1993), An accurate parameterization of the radiative properties of water clouds suitable for use in climate models, *J. Clim.*, *6*, 728–742.

Kollias, P., E. E. Clothiaux, B. A. Albrecht, M. A. Miller, K. P. Moran, and K. L. Johnson (2005), The Atmospheric Radiation Measurement program cloud profiling radars: An evaluation of signal processing and sampling strategies, *J. Atmos. Oceanic Technol.*, *22*, 930–948.

Martin, G. M., D. W. Johnson, and A. Spice (1994), The measurement and parameterization of effective radius of droplets in warm stratocumulus clouds, *J. Atmos. Sci.*, *51*, 1823–1842.

McFarlane, S. A., and K. F. Evans (2004), Clouds and shortwave fluxes at Nauru. part II: Shortwave flux closure, *J. Atmos. Sci.*, *61*, 2602–2615.

McFarlane, S. A., K. F. Evans, and A. S. Ackerman (2002), A Bayesian algorithm for the retrieval of liquid water cloud properties from microwave radiometer and millimeter radar data, *J. Geophys. Res.*, *107*(D16), 4317, doi:10.1029/2001JD001011.

Paluch, I. R., and C. A. Knight (1984), Mixing and the evolution of cloud droplet size spectra in a vigorous continental cumulus, *J. Atmos. Sci.*, *41*, 1801–1815.

Pawlowska, H., and J.-L. Brenguier (2000), Microphysical properties of stratocumulus clouds during ACE-2, *Tellus, Ser. B*, *52*, 868–887.

Pontikis, C. A., and E. M. Hicks (1993), The influence of clear air entrainment on the droplet effective radius of warm maritime convective clouds, *J. Atmos. Sci.*, *50*, 2829–2900.

Slingo, A., and H. M. Schrecker (1982), On the shortwave radiative properties of stratiform water clouds, *Q. J. R. Meteorol. Soc.*, *108*, 407–426.

Stephens, G. L. (1978), Radiation profiles in extended water clouds. II: Parameterization schemes, *J. Atmos. Sci.*, *35*, 2123–2132.

Stephens, G. L., and C. M. R. Platt (1987), Aircraft observations of the radiative and microphysical properties of stratocumulus and cumulus cloud fields, *J. Clim. Appl. Meteorol.*, *26*, 1243–1269.

Stommel, H. (1947), Entrainment of air into a cumulus cloud, *J. Meteorol.*, *4*, 91–94.

Su, C.-W., S. K. Krueger, P. A. McMurtry, and P. H. Austin (1998), Linear eddy modeling of droplet spectral evolution during entrainment and mixing in cumulus clouds, *Atmos. Res.*, *47–48*, 41–58.

Warner, J. (1955), The water content of cumuliform cloud, *Tellus*, *7*, 449–457.

Warner, J. (1969), The microstructure of cumulus cloud. part I. General features of the droplet spectrum, *J. Atmos. Sci.*, *26*, 1049–1059.

W. W. Grabowski, NCAR, Boulder, CO 80307-3000, USA. (grabow@ucar.edu)

S. A. McFarlane, PNNL, Richland, WA 99352, USA. (sally.mcfarlane@pnl.gov)